Effects of temperature, oxygen level, ionic strength, and pH on the reaction of benzene with hydroxyl radicals in aqueous atmospheric systems

ARTICLE *in* JOURNAL OF ENVIRONMENTAL CHEMICAL ENGINEERING · DECEMBER 2013

DOI: 10.1016/j.jece.2013.07.023

3 AUTHORS, INCLUDING:

Franz Ehrenhauser
Louisiana State University Agricultural Center
21 PUBLICATIONS **99** CITATIONS
SEE PROFILE

Kalliat Valsaraj
Louisiana State University
232 PUBLICATIONS **3,641** CITATIONS
SEE PROFILE

Journal of Environmental Chemical Engineering 1 (2013) 822–830

Contents lists available at ScienceDirect

Journal of Environmental Chemical Engineering

journal homepage: www.elsevier.com/locate/jece

Effects of temperature, oxygen level, ionic strength, and pH on the reaction of benzene with hydroxyl radicals in aqueous atmospheric systems

Aubrey A. Heath, Franz S. Ehrenhauser *, Kalliat T. Valsaraj

Cain Department of Chemical Engineering, 110 Chemical Engineering, South Stadium Drive, Louisiana State University, Baton Rouge, LA 70803, USA

ARTICLE INFO

Article history:
Received 28 February 2013
Received in revised form 18 July 2013
Accepted 19 July 2013

Keywords:
Benzene
Hydroxyl radicals
Biphenyl
Ionic strength
pH
Fog

ABSTRACT

In order to assess the degradation of aromatic compounds in fog, the reaction of benzene with hydroxyl radicals was studied in a bulk aqueous system. The effects of temperature, oxygen content, ionic strength, and pH were investigated in a batch reactor by following the two main products, phenol and biphenyl. The reaction rate increased with temperature, but was not significantly affected by ionic strength and pH. The overall phenol yield also did not significantly change with the removal of oxygen from the system. Conversely, the formation of biphenyl was more favorable under conditions of low oxygen content, high ionic strength, and low pH. The pH of the solution decreased during the reaction due to the formation of oxidation products of phenol; thus, we found that biphenyl did not form in detectable concentrations unless the pH was at or below 4.50–4.80.

Introduction

Benzene is listed as a known human carcinogen by the United States Environmental Protection Agency (U.S. EPA), and it is an atmospheric pollutant resulting from both stationary sources, such as chemical and petrochemical industry emissions, biomass burning, solvent usage and mobile sources, such as automobile exhaust [1,2]. Approximately 11 megatons of benzene are emitted annually worldwide. In the United States, the mean atmospheric benzene concentration has declined 55% between 1994 and 2008, with concentrations typically below 2.6×10^{-2} μmol/m^3 [3,4]. Nevertheless, in developing areas such as Delhi, India, the atmospheric concentration of benzene is higher (0.43–2.2 μmol/m^3) [5]. Due to its environmental ubiquity, benzene and its derivatives have not only been observed in the gas phase, but also in atmospheric waters such as fog, ice, rain, and cloud [6,7]. The atmospheric waters can vary greatly in both pH and ionic strength (I). Differences in ionic strength and pH for typical atmospheric water sources are shown in Table 1.

Although aromatic compounds are stable, benzene is known to react easily with hydroxyl radicals in the gas phase ($k_{OH} = 4.3 \times 10^4$ μM^{-1}·min^{-1}), whereas it is much less reactive toward ozone ($k_{O_3} = 6.1 \times 10^{-6}$ μM^{-1} min^{-1}) and nitrate radicals ($k_{NO_3} = 4.0 \times 10^{-1}$ μM^{-1} min^{-1}) [26]. In the aqueous phase, the reaction of benzene with hydroxyl radicals is also favorable ($k_{OH} = 4.7 \times 10^5$ μM^{-1} min^{-1}) [27,28].

The reaction of benzene with hydroxyl radicals has been explored extensively, particularly in the gas phase [2,29–32]. The reaction in aqueous solutions has also been studied, but many systems describe the kinetic evaluation of the photo-degradation of benzene by UV/hydrogen peroxide or other oxidative methods for wastewater treatment with minimal emphasis on additional product formation [33–36]. Our study also utilizes the photo-generation of hydroxyl radicals by UVB irradiation of hydrogen peroxide, but it emphasizes the formation of benzene's oxidative products: phenol and biphenyl. The formation of phenol has been studied extensively [2,29,30,37–41], whereas the kinetics of biphenyl formation has not been given much attention. Moreover, most previous work that describes biphenyl as a product of benzene with hydroxyl radicals focuses on Fenton's reagent system [38–40], which does not necessarily pertain to atmospheric conditions. Biphenyl, although not classified as a human carcinogen, is an irritant and toxin that affects the eyes, skin, kidneys, liver, and the central nervous system [42].

In this work, the photo-oxidation of benzene by hydroxyl radicals formed from hydrogen peroxide and UVB radiation is monitored in the bulk aqueous phase representing atmospheric droplets and advanced oxidation processes. Hydrogen peroxide is present in the natural environment in liquid aerosols, such as fog and clouds with typical concentrations of 0.3–3 μM [43–45]. Since

* Corresponding author. Tel.: +1 225 578 1426.
E-mail address: fehren1@tigers.lsu.edu (F.S. Ehrenhauser).

2213-3437/$ – see front matter © 2013 Elsevier Ltd. All rights reserved.
http://dx.doi.org/10.1016/j.jece.2013.07.023

Table 1
Ionic strength and pH in various atmospheric waters [8–25].

Type of solution	Ionic strength, I (eq./L)	pH
Seawater	0.7	7.5–8.5
Lake water	$1–8 \times 10^{-4}$	4.2–8.5
Rainwater	2×10^{-4}	4.3–5.6
Fog water	$1.1–78 \times 10^{-3}$	2.4–7.2
Cloud water	$9–12 \times 10^{-4}$	2.3–7.2

there is an apparent gap in the knowledge of the kinetics of biphenyl formation, we investigated the factors that influence the formation of both phenol and biphenyl: viz., temperature, oxygen content, ionic strength, and pH. These parameters, among others, determine the physico-chemical environment in atmospheric droplets such as fog and clouds, where the pH and ionic strength can vary from 2.3 to 7.2 and 0.09 to 78.0×10^{-3} eq./L, respectively (see Table 1) [11–15]. In atmospheric droplets, reactions are not only determined by the bulk phase conditions, but also by the surface reactions on the droplets. The surface pH is different from the bulk-phase pH; however, whether the surface is more acidic or basic than the bulk fluid is controversial [46–49]. The surface is also known to have an affinity for both aromatic compounds and hydroxyl radicals [50–54], which could influence compound fate given the large specific surface area of fog and clouds [55]. The present work is focused on the bulk aqueous phase and evaluates the effects of temperature, oxygen content, ionic strength, and pH on the photo-oxidation of benzene. These results will serve as the comparison basis for our future work on surfaces of atmospheric droplets.

Materials and methods

For experiments testing the effect of temperature (10–32 °C) on benzene degradation, LC–MS grade water (Burdick & Jackson, Muskegon, MI, USA) was used as received. The ionic strength of solutions was adjusted using sodium chloride (Mallinckrodt Baker, Inc., Phillipsburg, NJ, USA) prepared with LC–MS grade water (I = 0–1.7 eq./L). In order to model environmental conditions typical of fog water, the pH was adjusted using either sodium hydroxide (Mallinckrodt Baker, Inc., Phillipsburg, NJ, USA) or hydrochloric acid (Mallinckrodt Baker, Inc., Phillipsburg, NJ, USA). pH was measured with a pH meter (Oakton Acorn Series pH 6, Oakton Instruments, Vernon Hills, IL, USA) and either a ROSS Ultra Combination pH Electrode (ThermoScientific, Beverly, MA, USA) or a PHR-146B Micro Combination pH Electrode (Lazar, Los Angeles, CA, USA). Each aqueous solution was either saturated with UHP-grade air (Air Liquide America L.P., Houston, TX, USA) or degassed with UHP-grade helium (Air Liquide America L.P., Houston, TX, USA) for at least 2 h.

For each experiment, a solution with a benzene concentration of 13.2 mM was prepared from ACS grade benzene (Fisher Scientific, Fair Lawn, NJ, USA) and the previously described aqueous solution (pure, ionic strength adjusted, or pH adjusted). Since this concentration of benzene is much higher than what is seen in the environment, we performed separate experiments using solutions with a benzene concentration of 40.7 μM to investigate if the results from higher concentration experiments could be extrapolated down to lower levels.

30% (w/w) hydrogen peroxide (EMD Chemicals, Inc., Gibbstown, NJ, USA) was diluted to a 1% (w/w) solution in LC–MS grade water. We determined the actual concentration of hydrogen peroxide by iodometric titration with sodium thiosulfate (EMD Chemicals, Inc., Gibbstown, NJ, USA), standardized with potassium iodate (Mallinckrodt Chemical Works, New York, USA), and a 1% (w/w) starch (Acros Organics, NJ, USA) indicator solution. To determine the hydroxyl radical concentration in the system [56,57], we generated solutions of various initial concentrations of benzene (0.52–13.2 mM) in different reaction media: air-saturated, oxygen-free, ionic strength of 0.6-eq./L (neutral, pH = 6.23), and ionic strength of 0.6-eq./L (acidic, pH = 3.38). This value of ionic strength is about an order of magnitude higher than the typical ionic strength of fog water, and was chosen to evaluate how a significant increase in ionic strength affects the overall production of hydroxyl radicals. The values of pH tested were in the range typical of fog water.

We conducted all experiments in a batch reactor, schematically shown in Supplemental material, Section A.1, Fig. A.1. An insulated aluminum box housed two UVB light bulbs (15 W, 275–390 nm, UVP LLC, Upland, CA, USA) and the reaction vial. The light intensity is 1.3×10^3 W/m^2 at the bottom of the reaction vial. The wavelength range of the light bulbs covered the highly energetic UVB range of the solar spectrum and compares to solar radiation existing in the atmosphere. Since the UVB light bulbs generated heat, the reactor housing and vial were kept at constant temperature with the help of a cool, compressed air stream channeled in between the two light bulbs and a copper cooling coil connected to an external chiller (Model #RCB300, Hoefer Scientific Instruments, USA) that was beneath the two light bulbs. Unless otherwise noted, the reactor temperature was kept constant at 23 ± 1 °C.

The photochemical reaction was carried out in clear 27.5-mm × 70-mm borosilicate vials (Qorpak, Bridgeville, PA, USA), transparent to UVB radiation (cutoff wavelength: 300 nm). 30 mL of the appropriate benzene solution was used with minimal headspace in the vial. The vial was then wrapped in aluminum foil to prevent UVB light penetration and was held in place inside the reactor for 2 h to equilibrate at the desired temperature. Thereupon, we removed the foil and added 320 μL of the 1% hydrogen peroxide solution, resulting in a H_2O_2 concentration of 3.20 mM. The post-reaction hydrogen peroxide concentration, determined by iodometric titration, did not change significantly over the course of the reaction.

The solution was kept stirred by a magnetic stir bar throughout the experiment. 100 μL samples were taken at given intervals for analysis. These samples were withdrawn with a syringe through the cap septum. Each experiment was conducted in triplicate. The samples were all analyzed using an Agilent 1100 HPLC system. A description of the complete HPCL analysis is given in the Supplemental material, Section A.2. A typical chromatogram is depicted in Fig. A.2.

Results and discussion

Proposed reaction scheme

Fig. 1 shows the proposed reaction scheme of benzene reacting with hydroxyl radicals. In both the gas and aqueous phases, hydroxyl radicals react (rate constant k_p) with benzene (**1**) to form the hydroxycyclohexadienyl radical (**2**) [30,32,38–41,58] as seen in Fig. 1. This resonance-stabilized radical has four potential reaction pathways resulting in two main products: phenol (**4**) and biphenyl (**6**).

In the gaseous atmosphere, the dominant route for the hydroxycyclohexadienyl radical (**2**) is the reaction (rate constant k_{B3}) with oxygen to form the hydroxycyclohexadienyl peroxyl radical (**3**) [29,30,32,59]. This radical then decomposes to form phenol (**4**) and a hydroperoxyl radical [30,32,38–41]. Another potential route for phenol formation is the reaction of a hydroxycyclohexadienyl radical (**2**) with a hydroxyl radical (rate constant k_{B2}) [40]. Phenol (**4**) can also form through the disproportionation (rate constant k_{B1}) of two hydroxycyclohexadienyl radicals (**2**)

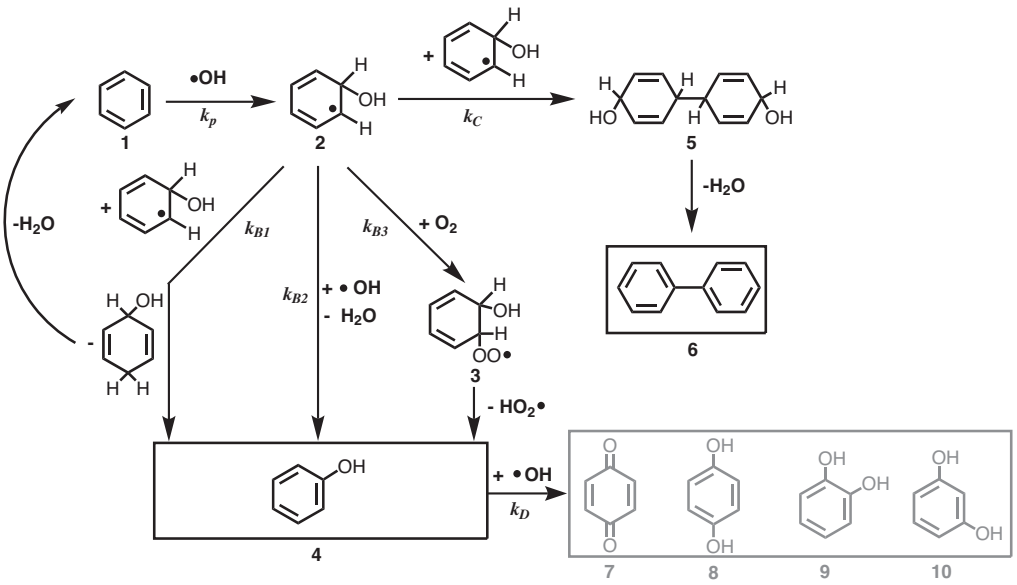

Fig. 1. Different reaction pathways for the photo-oxidation of benzene in water.

[38–40]. Phenol can be further oxidized to other organic products such as 1,4-benzoquinone (**7**), hydroquinone (**8**), catechol (**9**), and resorcinol (**10**) [37]. Some of these products, such as 1,4-benzoquinone ($pK_A = 4.0$) and further oxidation products [60], are more acidic than phenol ($pK_A = 9.95$) [61], which causes a decrease in solution pH.

In a second possible reaction pathway, two hydroxycyclohexadienyl radicals can dimerize (rate constant k_C) to form 4,4′-bishydroxycyclohexadiene (**5**) and its isomers, 2,4′-bishydroxycyclohexadiene and 3,4′-bishydroxycyclohexadiene (not shown in Fig. 1). These intermediate structures dehydrate to form another product, biphenyl (**6**) [38–40].

Determination of hydroxyl radicals

Following previous work [14,56,57], it is assumed that a steady state hydroxyl radical concentration is established during the UVB irradiation of a hydrogen peroxide solution. Benzene is used as a probe molecule and its main product, phenol, is followed throughout the reaction to determine the following quantitative parameters: P_{OH} (μM min^{-1}), the photochemical rate of production of hydroxyl radicals, $[OH]'_{ss}$ (μM), the steady state hydroxyl radical concentration, and k'_{np} (min^{-1}), the apparent first order rate constant for reactions of the hydroxyl radical not leading to phenol.

P_{OH}, k'_{np}, and $[OH]'_{ss}$ were found for the following solutions at 23 °C: air-saturated, oxygen-free, ionic strength of 0.6-eq./L (neutral, pH = 6.23), and ionic strength of 0.6-eq./L (acidic, pH = 3.38). The relevant equations are shown in the Supplemental material, Section A.4, Eqs. (A16)–(A19). Results for P_{OH}, k'_{np}, and $[OH]'_{ss}$ are shown in Table 2.

Table 2 shows that P_{OH} is highest for the acidic solution and the oxygen-free solution and lowest in the air-saturated case. Based on the results from [57], we calculated that P_{OH} for fog waters in Davis, CA ranged from 0.015 ± 0.003 to 0.16 ± 0.06 μM min^{-1}. Likewise, it was found that the photoformation rates of hydroxyl radicals in cloud waters, normalized to midday equinox sunlight, from Whiteface Mountain, NY ranged from 0.0078 to 0.050 μM min^{-1} [14]. Both fog water and cloud water show lower values of P_{OH} than the values found in this work due to the higher concentrations of both hydrogen peroxide and benzene used in the solution.

It is also clear from Table 2 that k'_{np} is highest for the solutions with an ionic strength of 0.6-eq./L and lowest for the air-saturated solution. This shows that a larger proportion of reactions lead to products other than phenol in solutions with high ionic strengths. An ionic strength of 0.6-eq./L is higher than what is typical of fog waters [10–13]. Since more ions are present, more interactions of the hydroxyl radical with other species are expected in these high ionic strength solutions, as shown in the high values for k'_{np}. The apparent first order •OH rate constant with other species is also lower in natural fog waters ($0.68 \pm 0.28 \times 10^6$–$1.9 \pm 0.09 \times 10^6$ min^{-1}) than in our experiment [57], due to the higher concentrations examined in our work.

However, the steady state hydroxyl radical concentrations, $[OH]'_{ss}$, found in this study were of the same order of magnitude observed in fog waters, $[OH]'_{ss} = 5.7 \pm 0.15 \times 10^{-10}$ μM [57]. Thus even though more radicals are produced (larger values for P_{OH}), the steady state hydroxyl radical concentration is not affected. Instead, hydroxyl radicals react with benzene at a proportionately larger rate and thus give a higher product yield. Only in the oxygen-free solution the steady state hydroxyl radical concentration was 56.6% higher in comparison to the air-saturated solution. In an air-saturated solution, hydrogen peroxide competes with oxygen, thus generating a lower steady-state hydroxyl radical concentration than in the oxygen-free solution.

Table 2
P_{OH} and k'_{np} for air-saturated, oxygen-free, $I = 0.6$ eq./L (neutral), and $I = 0.6$ eq./L (acidic) solutions of benzene (13.2 mM).

Type of solution	P_{OH} (μM min^{-1})	k'_{np} (min^{-1})	$[OH]'_{ss}$ (μM)
Air-saturated	1.24 ± 0.078	$7.43 \pm 3.9 \times 10^7$	$2.16 \pm 0.051 \times 10^{-10}$
Oxygen-free	1.62 ± 0.24	$1.50 \pm 1.1 \times 10^8$	$3.38 \pm 0.25 \times 10^{-10}$
$I = 0.6$ eq./L, Neutral	1.42 ± 0.097	$4.24 \pm 1.4 \times 10^8$	$2.19 \pm 0.073 \times 10^{-10}$
$I = 0.6$ eq./L, Acidic	1.64 ± 0.35	$6.34 \pm 15 \times 10^8$	$2.42 \pm 0.056 \times 10^{-10}$

Kinetic evaluation

We derived kinetic expressions for both phenol and biphenyl, Eqs. (1) and (2), respectively, based on the overall mechanism of the reaction of benzene with hydroxyl radicals (see Supplemental material, Section A.3).

$$\frac{C_B}{C_{A0}} = \frac{k_p[OH]_{ss}'}{k_D[OH]_{ss}'}\left(1 - e^{-k_D[OH]_{ss}'t}\right) = \frac{k_p'}{k_D'}(1 - e^{-k_D't}) \quad (1)$$

$$\frac{C_C}{C_{A0}} = 2\left(\frac{k_p[OH]_{ss}'}{k_{B2}[OH]_{ss}' + k_{B3}C_{O_2}}\right)^2 k_C C_{A0} t = k_C' C_{A0} t \quad (2)$$

where C_{A0} is the initial concentration of benzene, C_B is the concentration of phenol, C_C is the concentration of biphenyl, $[OH]'_{ss}$ is the steady state •OH concentration in the presence of benzene, C_{O_2} is the concentration of oxygen in solution, t is time, k_p is the rate constant of the reaction of benzene with hydroxyl radicals, k_D is the rate constant of the reaction of phenol with hydroxyl radicals, k_{B2} is the rate constant of the reaction of hydroxycyclohexadienyl radical with a hydroxyl radical, k_{B3} is the rate constant for the reaction of the hydroxycyclohexadienyl radical with oxygen, and k_C is the rate constant for biphenyl formation from dimerization.

It should be noted that the concentration of both benzene (13.2 mM) and hydrogen peroxide (3.2 mM) used in these experiments are higher than what typically exists in the environment. We used higher concentrations so that products that form in low concentrations, such as biphenyl, could be followed throughout the experiment, thus allowing for a more reliable analysis within this model study. Even in a polluted urban environment such as Delhi, India, with an atmospheric concentration of benzene of 0.43–2.2 μmol/m^3 [5], the air–water partition coefficient [62] would estimate an aqueous concentration of benzene during a fog event of approximately 0.012 μM. However, higher cloud water concentrations than Henry's Law predicts of toluene, ethyl benzene, and xylene have been observed [63]. This suggests that the fog water concentration of benzene could be higher than the Henry's Law constant estimate.

In order to test the effect of reactant concentration, we performed additional experiments with lower concentrations of both benzene (40.7 μM) and hydrogen peroxide (3.3 μM). Similar to all other experiments in this study, the concentration of benzene in this experiment is greater than the concentration of hydrogen peroxide; hence, the benzene concentration remained constant throughout the reaction.

When we compared initial rates (R_i) of the high and low concentration experiments, we found that at the higher concentration, the initial rate ($R_i = 9.85 \pm 0.45 \times 10^{-5}$) surpassed the one of the low concentration experiment ($R_i = 2.06 \pm 0.10 \times 10^{-5}$) by a factor of 4.77. Likewise, the ratio of the product of the initial concentration of the reactants in the high concentration experiment to the product of the initial concentration of the reactants in the low concentration experiment is 3.00. Thus, the product ratio is kinetically related to the rate ratio, as expected. Had these two ratios differed significantly from each other, the mechanism would not correspond to both higher and lower concentrations. However, based on these observations, we can conclude that even though the concentration levels in this study exceed usual environmental conditions, the mechanism drawn from our experiments will be applicable at environmentally relevant concentrations.

Effect of temperature

We calculated three apparent rate constants, k'_p, k'_D, and k'_C, and the overall yield for all temperatures. From 10 to 32 °C, the yield for phenol increased by 67.4%, k'_p increased by a factor of 3.8, and k'_D increased by a factor of 6.0. The apparent activation energy for the reaction of benzene with hydroxyl radicals and phenol with hydroxyl radicals was 50.3 ± 2.5 and 63.3 ± 2.3 kJ/mol, respectively, as obtained from the respective apparent rate constant variations with temperature. Fig. 2 shows the linear dependence of biphenyl yield on temperature, ranging from 15 to 32 °C. The apparent activation energy for biphenyl was 83.6 ± 34 kJ/mol. The error associated with the activation energy of biphenyl is large because biphenyl was only observed in the higher temperature experiments (biphenyl is below the limit of detection at 10 °C and only detectable at 180 min at 15 °C) and therefore had less data points associated to it than phenol, as seen in Fig. 2.

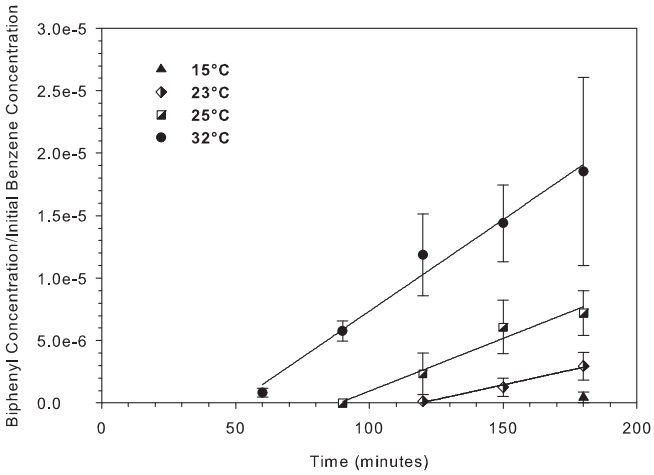

Fig. 2. Dependence of biphenyl yield on temperature (I = 0 eq./L).

Effect of oxygen

Fig. 3 shows the concentration of benzene, phenol, and biphenyl, each plotted against time for both the air-saturated solution and the oxygen-free solution.

It is apparent that the concentration of benzene remains approximately constant throughout the reaction. This is reinforced by the low product yields of both phenol (2.4%) and biphenyl (0.0019%). However, it is also clear that phenol has a 5% increase in yield in the oxygen-free solution compared to the air-saturated solution, and is coupled with a 124% increase in apparent rate constant for phenol degradation. This can be explained by the increased production of hydroxyl radicals and steady state hydroxyl radical concentration in the oxygen-free solution ($P_{OH} = 1.62 \pm 0.20$ μM min^{-1}; $[OH]'_{ss} = 3.38 \pm 0.25 \times 10^{-10}$ μM) compared to the air-saturated solution ($P_{OH} = 1.24 \pm 0.080$ μM min^{-1}; $[OH]'_{ss} = 2.16 \pm 0.051 \times 10^{-10}$ μM). Thus, there is a 30.6% increase in P_{OH} and a 56.48% increase in $[OH]'_{ss}$. Since $[OH]'_{ss}$ is known for these experiments, a more detailed description of the rate constants can be obtained, as seen with k_p and k_D in Table 3.

k_p decreases by 8.7% and k_D increases by 43.3% in the oxygen-free solution compared to the oxygen-saturated solution. However, the apparent rate constants, k'_p and k'_D, are 44.1% and 41.4%, respectively higher in the oxygen-free solution. In solution, the reaction of the hydroxycyclohexadienyl radical with oxygen ($k_{B3} = 3.0 \pm 0.4 \times 10^4$ μM^{-1} min^{-1}) is the favored reaction pathway in the presence of oxygen [42]. Disproportionation is less likely to occur because of steric hindrance [16]. However, when oxygen is absent, other reaction pathways do become significant. Phenol yield does not significantly change when oxygen is removed from the

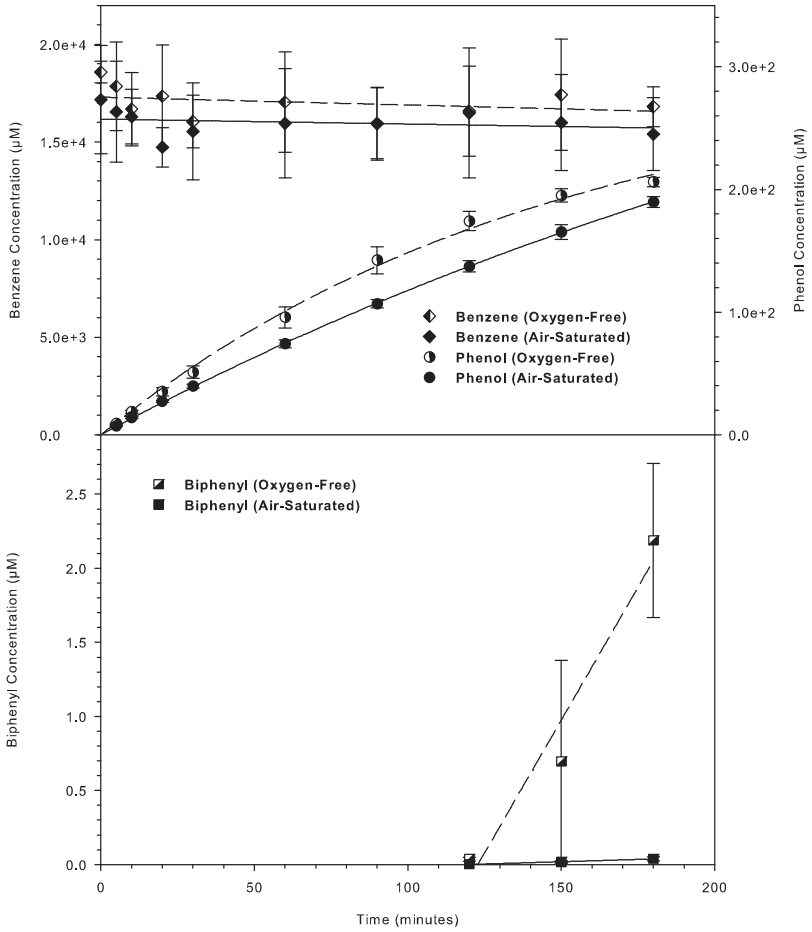

Fig. 3. Concentration of benzene, phenol, and biphenyl during the reaction in an air-saturated or an oxygen-free solution (T = 23 °C, I = 0 eq./L).

system. This shows that even though $[OH]'_{ss}$ increases by 56.5% in the oxygen-free solution, there is also an increase in both k'_p (formation of the hydroxycyclohexadienyl radical) and k'_D (destruction of phenol) (Eq. (1)); thus, we only observe a 5% increase in phenol yield.

Biphenyl yield increased by a factor of 50 in the oxygen-free solution when compared to the air-saturated solution. The substantial increase in biphenyl yield can be explained with a closer look at the kinetic evaluation. From the kinetic evaluation of the proposed mechanism (see Supplemental material, Section A.3), we have:

$$k'_C = 2\left(\frac{k_p[OH]_{ss}{}'}{k_{B2}[OH]_{ss}{}' + k_{B3}C_{O_2}}\right)^2 k_C \tag{3}$$

For the experiment where oxygen is removed ($C_{O_2} \sim 0$), k'_C is simplified and rearranged as follows,

$$\frac{k_C}{k_{B2}^2} = \frac{k'_{C,O_2 Free}}{2k_p^2} \tag{4}$$

For the oxygen-saturated experiment, no terms can be removed from Eq. (3). However, we know $[OH]'_{ss}$, k'_C, and k_p from experiment and C_{O_2} [64] and k_{B3} [58] from literature. Hence, between Eqs. (3) and (4) there are only two unknowns: k_C and k_{B2}. Solving this system of equations, allows us to estimate both constants: $k_{B2} = 5.32 \times 10^{15}$ and $k_C = 1.45 \times 10^{10}$ μM^{-1} min^{-1}. Even though the calculated rate constants associated with the hydroxyl radical are high, $[OH]'_{ss}$ is much lower than C_{O_2}; hence, the ratio of $(k_{B3}C_{O_2})$:$(k_{B2}[OH]'_{ss})$ is 1.2×10^5:1. Therefore, when oxygen is present in the system, the reaction pathway of phenol formation from oxygen is dominant over all other pathways [39–41]. By inserting the calculated rate constants, k_p, k_{B2}, k_{B3}, and k_C, and the values of C_{O_2} (268 μM) and $[OH]'_{ss}$ (2.16 ± 0.051 μM for the air-saturated solution) into the k'_C expression, we find that $k'_{C,O_2 Free}$ is 1.93×10^{-10} μM^{-1} min^{-1} and $k'_{C,O_2 Sat}$ is 3.57×10^{-12} μM^{-1} min^{-1}. The ratio of $(k'_{C,O_2 Free} : k'_{C,O_2 Sat})$ is 54:1; hence, this explains why the biphenyl yield increases by a factor of 50 in the oxygen-free solution when compared to the air-saturated solution (Fig. 3).

Thus the enhancement of yield and apparent reaction rate constant for phenol and biphenyl in the oxygen-free solution can be partly attributed to the increased hydroxyl radical concentration. Removing oxygen eliminates a major reaction pathway, allowing for more hydroxycyclohexadienyl-radical–hydroxycyclohexadienyl-radical interactions, and thus more biphenyl formation than in an oxygen-saturated solution.

Table 3
$[OH]'_{ss}$, k'_p, k_p, k'_D and k_D for oxygen-saturated and oxygen-free solutions of benzene (13.2 mM, T = 23 °C).

Type of solution	$[OH]'_{ss}$ ($\times 10^{10}$) (μM)	k'_p ($\times 10^4$) (min^{-1})	k_p ($\times 10^{-5}$) (μM^{-1} min^{-1})	k'_D ($\times 10^3$) (min^{-1})	k_D ($\times 10^{-7}$) (μM^{-1} min^{-1})
Air-saturated	2.16 ± 0.051	1.02 ± 0.050	4.73 ± 0.26	2.90 ± 0.10	1.34 ± 0.056
Oxygen-free	3.38 ± 0.25	1.47 ± 0.19	4.35 ± 0.64	4.10 ± 0.20	1.92 ± 0.25

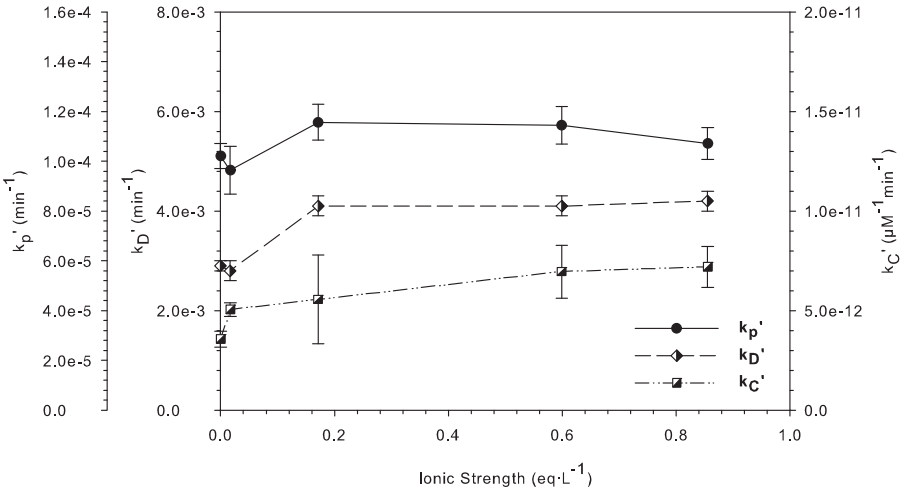

Fig. 4. Dependence of ionic strength on apparent rate constants, k'_P, k'_D, and k'_C (T = 23 °C).

Effect of ionic strength

The effect of ionic strength was tested to observe the differences between fresh water and moderate ionic strength environments such as atmospheric fog waters [10–13]. The lower ionic strength values correspond to conditions similar to those found in fog water, 0.0011 eq./L≤I≤0.078 eq./L, whereas the higher values of ionic strength, although not typical in the natural environment, were examined in order to see the extent of the effect ionic strength has on the degradation of benzene. Fig. 4 shows the observed rate constants, k'_P, k'_D, and k'_C, at each ionic strength value.

Within the bounds of error, k'_P experiences no significant change over this ionic strength range. Therefore, the reaction of benzene with hydroxyl radicals is not significantly affected by increased ionic strength in the system. On the other hand, there is a 41% increase in k'_D up to 0.17-eq./L, but no significant change in k'_D between a 0.17-eq./L and 0.86-eq./L solution. Similarly, k'_C (biphenyl formation) follows a similar trend (49% increase) as k'_D (phenol degradation). The rate increased (29%) between 0.17-eq./L and 0.86-eq./L solution.

Fig. 4 reveals that the rate constants of phenol degradation and biphenyl formation follow a similar trend as the solution increases in ionic strength. From the hydroxyl radical analysis, we observe a slight increase in P_{OH} (15%) and $[OH]'_{ss}$ (1.4%) in the 0.6-eq./L ionic strength solution in comparison to the air-saturated, zero ionic strength solution. However, there is a 41.4% and 95.0% increase in the apparent rate for phenol degradation and biphenyl production, respectively, in the 0.6-eq./L solution. The slight increase in $[OH]'_{ss}$ does not fully account for these increases in apparent rate. When the ionic strength of a solution increases, oxygen solubility decreases [64]. As seen in the oxygen-free experiments, removing oxygen in the system increases rate and yield for both phenol and biphenyl. When the solutions are saturated with oxygen, the 0.6-eq./L solution has 23% less oxygen dissolved than the 0-eq./L solution. Therefore, we evaluated the ratio of $k'_{C,I=0.6}$:$k'_{C,I=0}$ to be 1.80:1, or an 80.0% increase, which agrees with the 94.5% observed increase in the rate constant. This suggests that the decreased oxygen content in an increased ionic strength solution causes the biphenyl formation rate to increase. Since the apparent rate constants of phenol degradation and biphenyl formation follow the same trend, this implies that the reaction mechanism does not change with the increase of ionic strength.

Since typical fog water has an ionic strength in the range of 0.0011–0.078-eq./L [10–13], we expect to see slightly elevated apparent rate constants and yield for phenol and biphenyl in fog water solutions when compared to low ionic strength fresh waters [9,25].

Effect of pH

The initial pH of the 0-eq./L and 0.02-eq./L ionic strength solution was adjusted to both acidic and basic conditions in order to model the typical pH range of fog waters, 2.4–7.2 [10–13]. Three different cases were examined: acidic (HCl addition), neutral (no adjustment), and basic (NaOH addition). Fig. 5 shows the apparent rate constants, k'_P, k'_D, and k'_C, for phenol and biphenyl at the three pH values tested at each value of ionic strength.

Fig. 5 demonstrates that k'_P does not change significantly for both cases of ionic strength. This finding agrees with the previously observed results of the ionic strength experiments (see section "Effect of ionic strength"), which started at a neutral initial pH. The apparent rate constant for phenol degradation reveals no change in the zero ionic strength solution when the initial pH is acidic or neutral; the apparent rate constant decreases by 21.7% when the initial pH is basic. For the 0.02-eq./L ionic strength solution, there is no significant change in the apparent rate constant within the error bounds. On the other hand, k'_C increases by 44.4% and 22.8% as the pH increases for the zero ionic strength solution and I = 0.02-eq./L solution, respectively. Similar to the ionic strength experiments, we also observe a higher apparent rate of biphenyl formation at higher ionic strengths due to the decreased oxygen content in these solutions.

Fig. 6 displays the dependence of biphenyl concentration with time for three different initial pH values. Under further examination of Fig. 6, we observed that the onset of biphenyl formation also depended on initial pH; hence, biphenyl was formed in detectable concentrations earlier for solutions with lower initial pH values. For the acidic solutions, we detected biphenyl at 5 min, the first data point post irradiation. Similarly, in neutral solutions, biphenyl first appeared at 60 min, and in the basic solutions, biphenyl first appeared at 90 min.

In each experiment, we also found that the pH of the solution decreased during the reaction; hence, the pH post reaction was always 4.32 ± 0.02, except when the initial pH was already acidic (e.g. 3.35). The pH in the initially acidic solutions did not decrease further. The general decrease in pH can be attributed to the formation of additional acidic products from the further oxidation of phenol [37].

When the pH was measured throughout the experiment, it was observed that a pH range of 4.50–4.80 is needed for biphenyl to

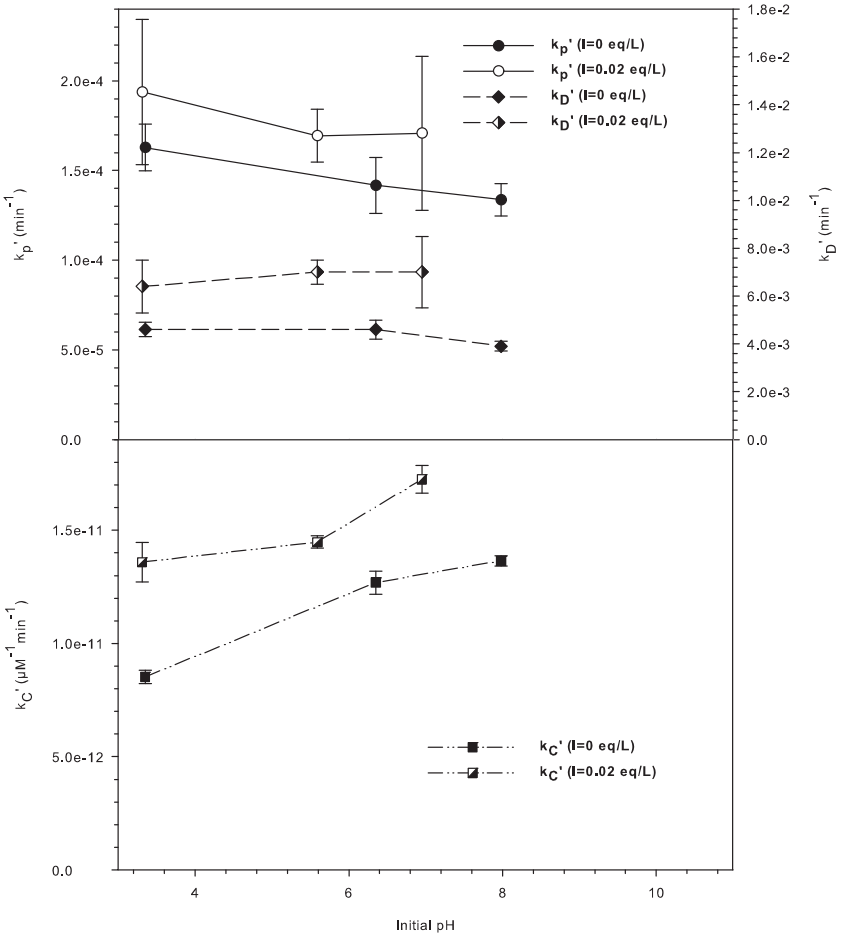

Fig. 5. Effect of pH on apparent rate constants, k'_p, k'_D, and k'_C, at I = 0 eq./L and I = 0.02 eq./L (T = 23 °C).

form in detectable concentrations. Since the initial pH of the acidic solution (pH = 3.35) is well below this pH value, biphenyl forms shortly after irradiation. The reaction takes longer to form biphenyl in detectable concentrations in the higher pH solutions (e.g. pH = 6.35 and 7.98) because additional acidic products must be formed before the lower pH range of 4.50–4.80 can be obtained.

The delayed onset of biphenyl formation was also observed at different temperatures. Biphenyl was not observed during the 10 °C experiment and was only observed after 3 h in the 15 °C experiment (Fig. 2). We did not detect biphenyl (limit of detection for biphenyl is 1.52×10^{-3} μM) until the phenol concentration was at least 139.7 ± 4.6 μM. At this concentration of phenol, enough of its oxidation products formed, which allowed for the pH to fall within the range favorable for biphenyl formation, 4.50–4.80. Because the maximum phenol concentration in the 10 °C experiment was only 108.3 ± 6.3 μM, this pH range was not obtained, and thus biphenyl did not form. Removing oxygen from the system did not affect the onset of biphenyl formation because the decrease in pH is not affected when oxygen is removed. Thus, the pH needed for the significant formation of biphenyl is reached at the same time in both air-saturated and oxygen-free solutions. The pH in the low concentration experiment remained constant throughout the reaction (pH = 5.64 ± 0.14), and thus we did not observe biphenyl in this experiment. We performed an additional low concentration experiment with an initial pH of 3.64 and biphenyl was observed, but only in very low concentrations.

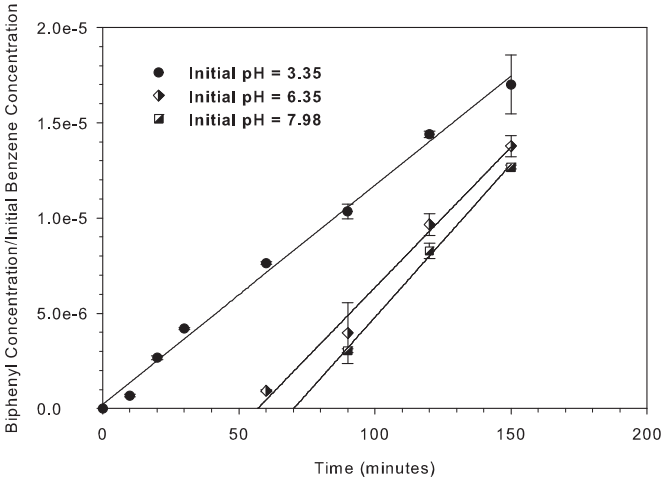

Fig. 6. Dependence of pH on biphenyl yield (T = 23 °C, I = 0 eq./L).

The effect of pH on biphenyl formation can be explained at a molecular level. In a bulk aqueous solution, photoionized benzene and water form benzene-water cluster cations ($[C_6H_6–(H_2O)_n]^+$, n = 1–23), where n is the number of water molecules [65]. Microscopic water clusters have a H_3O^+ ion core and formation of these clusters occurs in three phases: chain ($n \leq 10$), net ($10 \approx n \approx 20$), and cage ($n \geq 21$). In small water clusters ($n < 8$), a benzene moiety, such as a phenyl radical or a hydroxycyclohexadienyl radical, may directly coordinate to this ion core via a σ-type hydrogen bond. However, in bulk aqueous solutions (n = 21), water molecules form a distinct hydrogen bond network, which

pushes the benzene moiety toward the cluster surface [65]. This sheds light on why biphenyl formation is dependent on an acidic pH: when the pH is low in a bulk aqueous system, benzene moieties are forced outside of the solvent cage. Since there are more opportunities for benzene-benzene interactions, biphenyl formation can occur.

The immediate biphenyl formation under acidic conditions is interesting for atmospheric waters, such as fog waters, which have moderate ionic strengths and potentially low pH, especially at the air–water interface. This implies that favorable conditions are likely in the environment for biphenyl formation from benzene, which is enhanced by an increased ionic strength and a decreased pH. Since reactions within atmospheric droplets depend on conditions in the bulk phase and at the surface, the high specific surface areas provided by small droplets in the atmosphere can enhance the effect of surface reactions.

Conclusions

Benzene degradation by hydroxyl radicals (k'_p) is affected by temperature, but shows no significant difference in the ionic strength range (0–0.86-eq./L) and pH range (3.31–7.98) tested. However, salinity and pH were shown to affect both phenol degradation (k'_D) and biphenyl formation (k'_C). Removing oxygen from the solution increased the apparent rate constant and overall yield of phenol degradation by 124% and 5%, respectively, and biphenyl yield was increased by a factor of 50. When oxygen is saturated in solution, the reaction of oxygen with the hydroxycyclohexadienyl radical dominates because the concentration of oxygen is much greater than the steady state concentration of hydroxyl radicals. However, removing oxygen opens up the ability for additional reaction pathways to hold more significance. Hence, we observed a higher concentration of biphenyl in the oxygen-free solution than in the oxygen-saturated solution, and the overall yield of phenol did not significantly change because the other phenol formation pathways compensated for the removal of oxygen.

Increasing the ionic strength from 0-eq./L to 0.86-eq./L increased the rate of phenol degradation by 44.8% and the rate of biphenyl formation by 102%. Although ionic strength conditions as high as 0.86-eq./L are uncommon for the atmosphere, a 41.4% increase in phenol degradation and a 56.0% increase in biphenyl formation occurred in comparison of a 0-eq./L solution to a 0.17-eq./L solution, conditions which are representative of the environment. As ionic strength increases, the solubility of oxygen decreases; hence, the increase in apparent rate at higher ionic strengths is attributed to a decrease in oxygen in the system. As seen with the oxygen-free experiments, reaction pathways that generally are minimal in the presence of oxygen become more significant. Therefore, fog events, which exhibit moderate ionic strength, are expected to experience higher reaction rates than events with lower ionic strengths.

Adjusting the pH of the initial solution from basic (7.98, I = 0 eq./L or 6.98, I = 0.02 eq./L) to more acidic (3.35, I = 0 eq./L or 3.31, I = 0.02 eq./L) conditions had minimal effect on the overall apparent rate constant for both phenol and biphenyl. Although the pH may initially be more basic, the pH of the solution decreases over the span of the reaction due to the formation of acidic products from the oxidation of phenol. For example, the pH of an initial basic solution with 0 M ionic strength decreased from 7.98 to 4.33 over the span of the reaction. This decrease in pH coincides with the onset of biphenyl formation; hence, when the pH reaches a value in the range of 4.50–4.80, biphenyl forms in detectable concentrations. This dependence of biphenyl formation on acidic pH is important in atmospheric waters, such as fog water and cloud water, which are generally acidic. Due to the high specific surface area of liquid aerosols and the potential of the surface being more acidic than the bulk phase, biphenyl formation could be significant for the reaction of benzene with hydroxyl radicals in aqueous atmospheric aerosols.

Acknowledgements

Research funding for this work was provided by NSF Grant AGS-1106569. A special thanks to both Dr. William Brookshire and to Schlumberger for providing the William Brookshire Graduate Assistantship in Chemical Engineering and Schlumberger Assistantship Supplement, respectively, to Aubrey Heath.

Appendix A. Supplementary data

Supplementary data associated with this article can be found, in the online version, at doi:10.1016/j.jece.2013.07.023.

References

[1] U.S. EPA, Integrated Risk Information System (IRIS) on Benzene, Washington, DC, U.S. EPA, 2002.
[2] T. Berndt, O. Böge, Formation of phenol and carbonyls from the atmospheric reaction of OH radicals with benzene, Physical Chemistry Chemical Physics 8 (2006) 1205–1214.
[3] U.S. EPA, Data from the Air Quality System, Washington, DC, U.S. EPA, 2008.
[4] E. Borrás, L.A. Tortajada-Genaro, Secondary organic aerosol formation from the photo-oxidation of benzene, Atmospheric Environment 47 (2012) 154–163.
[5] A. Kumar, S.K. Tyagi, Benzene and toluene profiles in ambient air of Delhi as determined by active sampling and GC analysis, Journal of Scientific and Industrial Research 65 (2006) 252–257.
[6] G. Kos, P.A. Ariya, Volatile organic compounds in snow in the Quebec-Windsor Corridor, Journal of Geophysical Research: Atmospheres 115 (2010).
[7] S. Raja, R. Raghunathan, R.R. Kommalapati, X. Shen, J.L. Collett Jr., K.T. Valsaraj, Organic composition of fogwater in the Texas–Louisiana gulf coast corridor, Atmospheric Environment 43 (2009) 4214–4222.
[8] V.P. Aneja, C.S. Claiborn, R.L. Bradow, R.J. Paur, R.E. Baumgardner, Dynamic chemical characterization of montane clouds, Atmospheric Environment 24 (1990) 563–572.
[9] M.P. Anderson, C.J. Bowser, The role of groundwater in delaying lake acidification, Water Resources Research 22 (1986) 1101–1108.
[10] D.J. Jacob, J.M. Waldman, J.W. Munger, M.R. Hoffmann, Chemical composition of fogwater collected along the California coast, Environmental Science and Technology 19 (1985) 730–736.
[11] R.L. Brewer, R.J. Gordon, L.S. Shepard, E.C. Ellis, Chemistry of mist and fog from the Los Angeles urban area, Atmospheric Environment 17 (1983) 2267–2270.
[12] S. Fuzzi, M.C. Facchini, G. Orsi, G. Bonforte, W. Martinotti, G. Ziliani, P. Mazzalit, P. Rossi, P. Natale, M.M. Grosa, E. Rampado, P. Vitali, R. Raffaelli, G. Azzini, S. Grotti, The NEVALPA project: a regional network for fog chemical climatology over the PO Valley basin, Atmospheric Environment 30 (1996) 201–213.
[13] S. Raja, R. Raghunathan, X.Y. Yu, T. Lee, J. Chen, R.R. Kommalapati, K. Murugesan, X. Shen, Y. Qingzhong, K.T. Valsaraj, J.L. Collett Jr., Fog chemistry in the Texas–Louisiana Gulf Coast corridor, Atmospheric Environment 42 (2008) 2048–2061.
[14] B.C. Faust, J.M. Allen, Aqueous-phase photochemical formation of hydroxyl radical in authentic cloudwaters and fogwaters, Environmental Science and Technology 27 (1993) 1221–1224.
[15] J.B. Anderson, R.E. Baumgardner, V.A. Mohnen, J.J. Bowser, Cloud chemistry in the eastern United States, as sampled from three high-elevation sites along the Appalachian Mountains, Atmospheric Environment 33 (1999) 5105–5114.
[16] D.J. Jacob, J.W. Munger, J.M. Waldman, M.R. Hoffmann, The H_2SO_4–HNO_3–NH_3 system at high humidities and in fogs 1. Spatial and temporal patterns in the San Joaquin Valley of California, Journal of Geophysical Research 91 (1986) 1073–1088.
[17] S.V. Hering, D.L. Blumenthal, R.L. Brewer, A. Gertler, M. Hoffmann, J.A. Kadlecek, K. Pettus, Field intercomparison of five types of fog water collectors, Environmental Science and Technology 21 (1987) 654–663.
[18] Y.-H. Li, Seasalt and pollution inputs over the continental United States, Water, Air, and Soil Pollution 64 (1992) 561–573.
[19] F.J. Millero, The physical chemistry of seawater, Annual Review of Earth and Planetary Sciences 2 (1974) 101–150.
[20] K.C. Weathers, G.E. Likens, F.H. Bormann, S.H. Bicknell, B.T. Bormann, B.C. Daube, J.S. Eaton, J.N. Galloway, W.C. Keene, K.D. Kimball, W.H. McDowell, T.G. Siccama, D. Smiley, R.A. Tarrant, Cloudwater chemistry from ten sites in North America, Environmental Science and Technology 22 (1988) 1018–1026.
[21] A. Zirino, Measurement of the Apparent pH of Seawater with a Combination Microelectrode, Limnology and Oceanography 20 (1975) 654–657.
[22] Z. Li, V.P. Aneja, Regional analysis of cloud chemistry at high elevations in the eastern United States, Atmospheric Environment 26 (1992) 2001–2017.
[23] S. Fuzzi, G. Orsi, G. Nardini, M.C. Facchini, S. McLaren, E. McLaren, M. Mariotti, Heterogeneous processes in the Po Valley radiation fog, Journal of Geophysical Research 93 (1988) 11141–11151.

[24] M.C. Facchini, S. Fuzzi, M. Kessel, W. Wobrock, W. Jaeschke, B.G. Arends, J.J.M.Ö. Ls, A. Berner, I. Solly, C. Kruisz, G. Reischl, S. Pahl, A. Hallberg, J.A. Ogren, H. Fierlinger-Oberlinninger, A. Marzorati, D. Schell, The chemistry of sulfur and nitrogen species in a fog system A multiphase approach, Tellus B 44 (1992) 505–521.
[25] G.P. Hu, R. Balasubramanian, C.D. Wu, Chemical characterization of rainwater at Singapore, Chemosphere 51 (2003) 747–755.
[26] B.J. Finlayson-Pitts, J.N. Pitts, Chemistry of the upper and lower atmosphere, second ed., Academic Press, San Diego, CA, 2000.
[27] G.V. Buxton, C.L. Greenstock, W.P. Helman, A.B. Ross, Critical Review of rate constants for reactions of hydrated electrons, hydrogen atoms and hydroxyl radicals in aqueous solution, Journal of Physical and Chemical Reference Data 17 (1988) 513–886.
[28] D. Minakata, K. Li, P. Westerhoff, J. Crittenden, Development of a group contribution method to predict aqueous phase hydroxyl radical ($HO^{\bullet}$) reaction rate constants, Environmental Science and Technology 43 (2009) 6220–6227.
[29] R. Atkinson, S.M. Aschmann, J. Arey, W.P.L. Carter, Formation of ring-retaining products from the OH radical-initiated reactions of benzene and toluene, International Journal of Chemical Kinetics 21 (1989) 801–827.
[30] T.H. Lay, J.W. Bozzelli, J.H. Seinfeld, Atmospheric photochemical oxidation of benzene: benzene + OH and the benzene – OH adduct (hydroxyl-2,4-cyclohexadienyl) + O_2, Journal of Physical Chemistry 100 (1996) 6543–6554.
[31] T. Berndt, O. Böge, H. Herrmann, On the formation of benzene oxide/oxepin in the gas-phase reaction of OH radicals with benzene, Chemical Physics Letters 314 (1999) 435–442.
[32] S.Y. Grebenkin, L.N. Krasnoperov, Kinetics thermochemistry of the hydroxycyclohexadienyl radical reaction with O_2, Journal of Physical Chemistry A 108 (2004) 1953–1963.
[33] V. Goncharuk, N. Soboleva, A. Nosonovich, Photooxidative destruction of organic compounds by hydrogen peroxide in water, Journal of Water Chemistry and Technology 32 (2010) 17–32.
[34] D.W. Sundstrom, B.A. Weir, H.E. Klei, Destruction of aromatic pollutants by UV light catalyzed oxidation with hydrogen peroxide, Environmental Progress 8 (1989) 6–11.
[35] A.H.A.M. Daifullah, M.M. Mohamed, Degradation of benzene, toluene ethylbenzene and *p*-xylene (BTEX) in aqueous solutions using UV/H_2O_2 system, Journal of Chemical Technology and Biotechnology 79 (2004) 468–474.
[36] J.W. Kang, K.H. Lee, A Kinetic model of the hydrogen peroxide/UV process for the treatment of hazardous waste chemicals, Environmental Engineering Science 14 (1997) 183–192.
[37] A.K. De, S. Bhattacharjee, B.K. Dutta, Kinetics of phenol photooxidation by hydrogen peroxide and ultraviolet radiation, Industrial and Engineering Chemistry Research 36 (1997) 3607–3612.
[38] E.A. Karakhanov, S.Y. Narin, A.G. Dedov, On the mechanism of catalytic hydroxylation of aromatic hydrocarbons by hydrogen peroxide, Applied Organometallic Chemistry 5 (1991) 445–461.
[39] C.R.E. Jefcoate, J.R.L. Smith, R.O.C. Norman, Hydroxylation. Part IV. Oxidation of some benzenoid compounds by Fenton's reagent and the ultraviolet irradiation of hydrogen peroxide, Journal of the Chemical Society B: Physical Organic (1969) 1013–1018.
[40] J.R.L. Smith, R.O.C. Norman, 539. Hydroxylation. Part I. The oxidation of benzene and toluene by Fenton's reagent, Journal of the Chemical Society (Resumed) (1963) 2897–2905.
[41] C. Walling, R.A. Johnson, Fenton's reagent. V. Hydroxylation and side-chain cleavage of aromatics, Journal of the American Chemical Society 97 (1975) 363–367.
[42] U.S. EPA, Integrated Risk Information System (IRIS) on Biphenyl, Washington, DC, 1999.
[43] W.J. Cooper, R.G. Zika, R.G. Petasne, J.M.C. Plane, Photochemical formation of hydrogen peroxide in natural waters exposed to sunlight, Environmental Science and Technology 22 (1988) 1156–1160.
[44] B.C. Faust, Photochemistry of clouds fogs, and aerosols, Environmental Science and Technology 28 (1994) 216A–222A.
[45] T.E. Graedel, C.J. Weschler, Chemistry within aqueous atmospheric aerosols and raindrops, Reviews of Geophysics 19 (1981) 505–539.
[46] J.K. Beattie, A.M. Djerdjev, G.G. Warr, The surface of neat water is basic, Faraday Discussions 141 (2009) 31–39.
[47] V. Buch, A. Milet, R. Vácha, P. Jungwirth, J.P. Devlin, Water surface is acidic, Proceedings of the National Academy of Sciences 104 (2007) 7342–7347.
[48] P.B. Petersen, R.J. Saykally, Is the liquid water surface basic or acidic? Macroscopic vs. molecular-scale investigations, Chemical Physics Letters 458 (2008) 255–261.
[49] B. Winter, M. Faubel, R. Vácha, P. Jungwirth, Behavior of hydroxide at the water/vapor interface, Chemical Physics Letters 474 (2009) 241–247.
[50] J. Chen, F.S. Ehrenhauser, K.T. Valsaraj, M.J. Wornat, Uptake UV-photooxidation of gas-phase PAHs on the surface of atmospheric water films. 1. Naphthalene, Journal of Physical Chemistry A 110 (2006) 9161–9168.
[51] M. Roeselova, J. Vieceli, L.X. Dang, B.C. Garrett, D.J. Tobias, Hydroxyl radical at the air–water interface, Journal of the American Chemical Society 126 (2004) 16308–16309.
[52] C.D. Wick, L.X. Dang, Computational observation of enhanced solvation of the hydroxyl radical with increased NaCl concentration, Journal of Physical Chemistry B 110 (2006) 8917–8920.
[53] R. Vacha, P. Jungwirth, J. Chen, K. Valsaraj, Adsorption of polycyclic aromatic hydrocarbons at the air–water interface: molecular dynamics simulations and experimental atmospheric observations, Physical Chemistry Chemical Physics 8 (2006) 4461–4467.
[54] J. Chen, F.S. Ehrenhauser, K.T. Valsaraj, M.J. Wornat, in: K.T. Valsaraj, R.R. Kommalapati (Eds.), Adsorption and UV photooxidation of gas-phase phenanthrene on atmospheric films in Atmospheric Aerosols Characterization, Chemistry, Modeling, and Climate, Vol. 1005, Oxford University Press, Washington, DC, 2009, pp. 127–146.
[55] K.T. Valsaraj, Elements of Environmental Engineering: Thermodynamics and Kinetics, Taylor and Francis Group LLC, Boca Raton, 2009.
[56] X. Zhou, K. Mopper, Determination of photochemically produced hydroxyl radicals in seawater and freshwater, Marine Chemistry 30 (1990) 71–88.
[57] C. Anastasio, K.G. McGregor, Chemistry of fog waters in California's Central Valley: 1. In situ photoformation of hydroxyl radical and singlet molecular oxygen, Atmospheric Environment 35 (2001) 1079–1089.
[58] L.M. Dorfman, I.A. Taub, R.E. Buhler, Pulse radiolysis studies. I. Transient spectra and reaction-rate constants in irradiated aqueous solutions of benzene, Journal of Chemical Physics 36 (1962) 3051–3061.
[59] B. Bohn, C. Zetzsch, Gas-phase reaction of the OH-benzene adduct with O_2: reversibility and secondary formation of HO_2, Physical Chemistry Chemical Physics 1 (1999) 5097–5107.
[60] G.E. Adams, B.D. Michael, Pulse radiolysis of benzoquinone and hydroquinone. Semiquinone formation by water elimination from trihydroxy-cyclohexadienyl radicals, Transactions of the Faraday Society 63 (1967) 1171–1180.
[61] W.H. Brown, C.S. Foote, B.L. Iverson, E.V. Anslyn, B.M. Novak, Organic Chemistry, Cengage Learning, 2011.
[62] R.A. Ashworth, G.B. Howe, M.E. Mullins, T.N. Rogers, Air–water partitioning coefficients of organics in dilute aqueous solutions, Journal of Hazardous Materials 18 (1988) 25–36.
[63] J. Hutchings, M. Robinson, H. McIlwraith, J. Triplett Kingston, P. Herckes, The Chemistry of intercepted clouds in northern Arizona during the North American monsoon season, Water, Air, and Soil Pollution 199 (2009) 191–202.
[64] R. Battino, T.R. Rettich, T. Tominaga, The solubility of oxygen and ozone in liquids, Journal of Physical and Chemical Reference Data 12 (1983) 163–178.
[65] M. Miyazaki, A. Fujii, T. Ebata, N. Mikami, Infrared spectroscopy of size-selected benzene–water cluster cations $[C_6H_6\text{–}(H_2O)_n]^+$ (n = 1–23): Hydrogen Bond Network Evolution and Microscopic Hydrophobicity, Journal of Physical Chemistry A 108 (2004) 10656–10660.